

Supplementary Materials for
**Multomics analyses reveal *DARS1-AS1/YBX1*–controlled posttranscriptional
circuits promoting glioblastoma tumorigenesis/radioresistance**

Caishang Zheng *et al.*

Corresponding author: Yiwen Chen, ychen26@mdanderson.org, ywcus08@gmail.com; Ming Sun,
sunming348@hotmail.com

Sci. Adv. **9**, eadf3984 (2023)
DOI: 10.1126/sciadv.adf3984

The PDF file includes:

Supplementary Methods
Figs. S1 to S7
Legends for tables S1 to S6

Other Supplementary Material for this manuscript includes the following:

Tables S1 to S6

Supplementary Methods.

In vitro RNA pull-down

To perform in vitro RNA pull-down assay for DARS1-AS1 (NR_110199.1), we used the Pierce™ Magnetic RNA-Protein Pull-Down Kit (Thermo Fisher #20164) and adopted a published protocol, as described previously (PMID: 27659978). Briefly, the full-length DARS1-AS1 cDNA sequence was PCR-amplified with an addition of T7 promoter sequence to its 5' end (see primer sequences in Table S3). T7 RiboMAX™ Express Large-Scale RNA Production System (Promega #P1320) was used to produce full-length RNAs by in vitro transcription with the PCR-amplified T7-promoter-cDNA template, according to the manufacturer's instruction. Transcribed RNAs were purified using RNeasy Mini Kit (QIAGEN, # 74004) and desthiobiotin-labeled using Pierce RNA 3' End Desthiobiotinylation Kit (Thermo Fisher, # 20163). A total of 50 pmol desthiobiotin-labeled RNA was incubated with 50 μ L streptavidin magnetic beads for 30 min at room temperature with agitation. RLN buffer and protein lysis buffer were used to prepare cell extract from the U251 cells that were transfected with the vectors expressing GFP or GFP-tagged full length and truncation mutant YBX1. The streptavidin magnetic beads were then washed twice with an equal volume of 20 mM Tris buffer and incubated with prepared cell extract in protein-RNA binding buffer at 4 °C with agitation or rotation for 1 h. After washing 4 times with wash buffer, the RNA-binding protein complexes were eluted with elution buffer and analyzed with semi-quantitative RT-PCR or western blot.

Dual luciferase reporter assay

The wild-type 3'UTR of E2F1, CCND1, and FOXM1, or their mutant 3'UTR with deletion of YBX1 binding sites were synthesized (Twist Bioscience) and inserted downstream of the firefly luciferase transcriptional unit of pGL3 firefly luciferase reporter vector (Promega, #E1761). The pRL-TK vector (Promega, #E2241) was used as Renilla luciferase control reporter. The U251 cells were co-transfected with the reporter plasmid containing firefly luciferase fused to wild type or mutant 3'UTR sequences, pRL-TK plasmid (as internal control) and the negative control siRNA (siNC)/siRNA targeting DARS1-AS1/YBX1 for 24 h. The cells were then plated in 96-wells plate and cultured for another 48 h before being lysed for measuring luciferase activity. Dual luciferase reporter assay was performed using the Dual-Glo® Luciferase assay kit (Promega, #E2940), according to the manufacturer's instructions. Briefly, cells in 96-wells plate were incubated with 75 μ L Dual-Glo reagent for at least 10 min at room temperature. The plate was then loaded to the Synergy™ H1 Microplate Reader for firefly luciferase luminescence measurement. Following the completion of firefly luciferase luminescence measurement, another 75 μ L Dual-Glo® Stop & Glo® Reagent was added to each well and incubated for 10 min. The plate was then loaded to the Synergy™ H1 Microplate Reader for Renilla luciferase luminescence measurement. The luminescence was measured with a 10s of integration time and the gain setting at 135. The normalized luciferase activity data are represented as the ratio of firefly to Renilla luciferase luminescence.

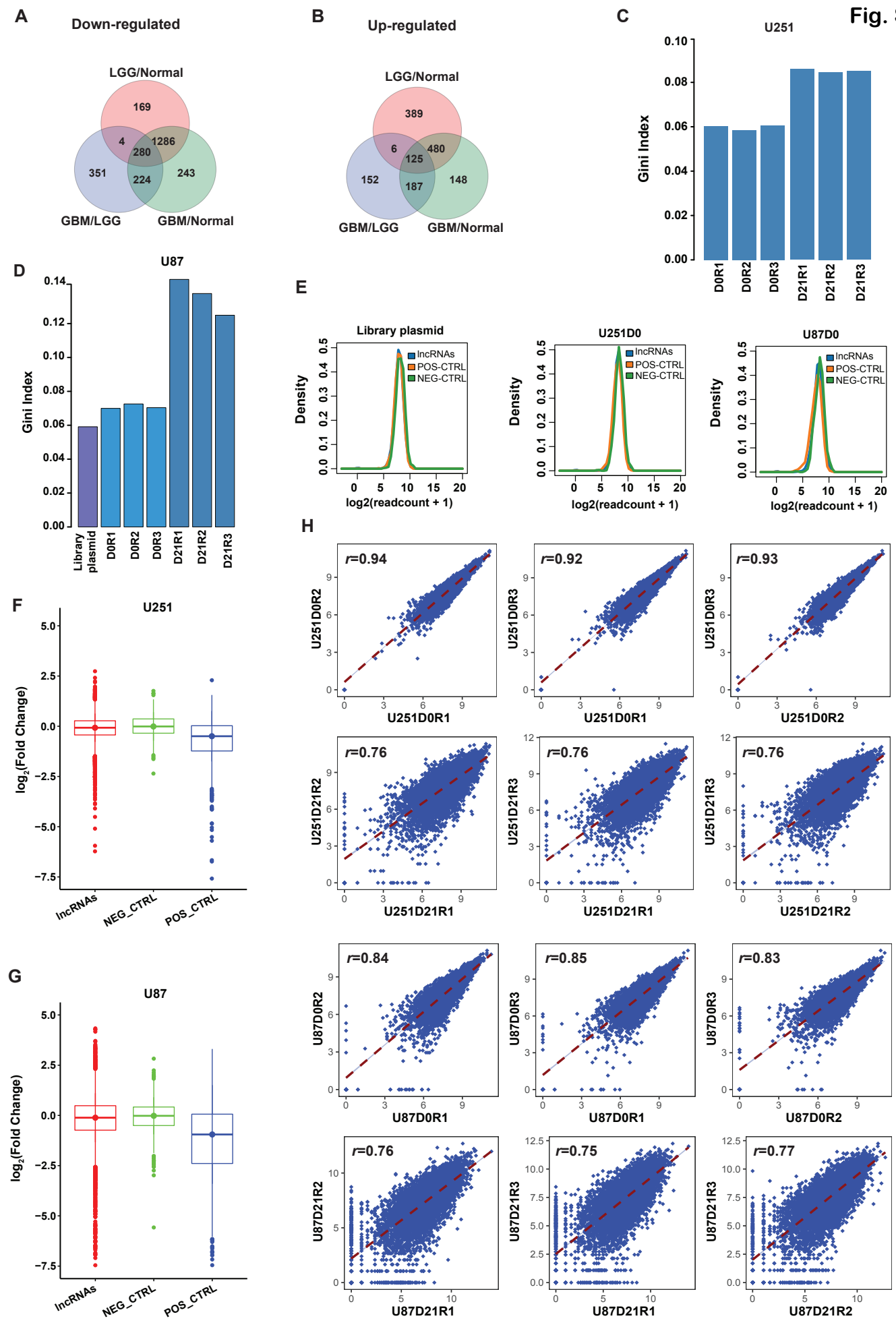


Figure S1. Venn diagrams showing the overlap of the significantly (A) up-regulated or (B) down-regulated lncRNA genes ($|\log_2\text{Fold-Change}| \geq \log_2(1.5)$, $FDR < 0.05$) from the following comparisons: GBM tumors vs. normal brain tissues (normal), low-grade glioma (LGG) vs. normal and GBM vs. LGG. Gini index characterizing the uniformity of the sgRNA coverage in the library plasmid or the libraries prepared from (C) U251 and (D) U87 cells on day 0 (D0) and day 21 (D21). (E) Density plots showing the distribution of the negative control (green)/positive control (orange) sgRNAs or the sgRNAs targeting the lncRNAs (blue) in the library plasmid, and the D0 libraries from U251 and U87 cells. Boxplots showing the $\log_2(\text{Fold-Change})$ between day 21 and day 0 for sgRNAs targeting the lncRNAs (red), the negative controls (green), and the positive control genes (blue) in (F) U251 and (G) U87 cells. (H) The scatter plots showing the correlations of sgRNA abundances between the three replicates of D0 and D21 libraries from U251 and U87 cells. The Pearson correlation coefficient was used to quantify the correlations and all the correlations are statistically significant ($P < 2.2 \times 10^{-16}$).

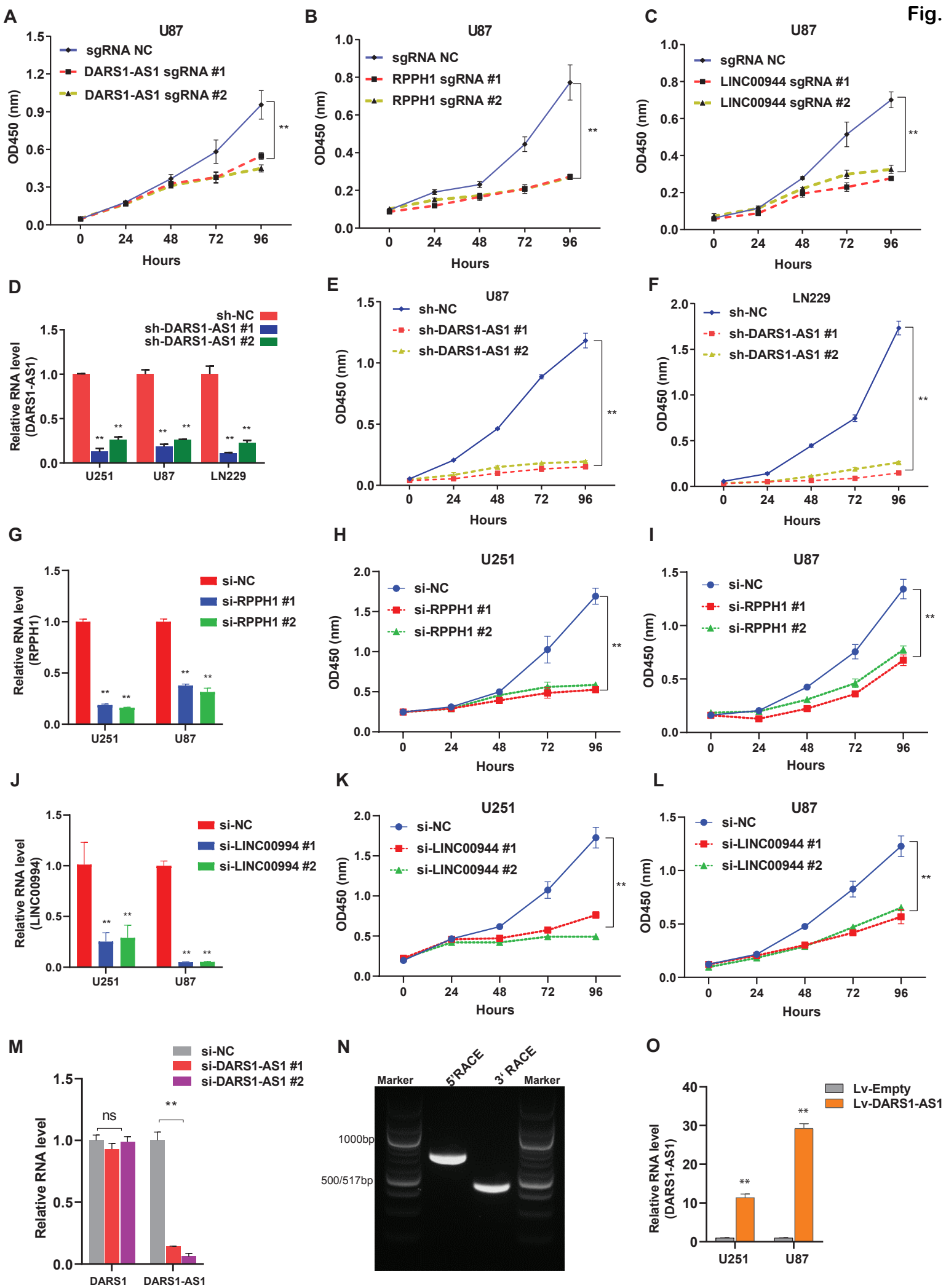


Figure S2. The growth of the U87 cells transduced with the negative control sgRNA (sg-NC)/sgRNAs targeting (A) DARS1-AS1, (B) RPPH1 or (C) LINC00944 was monitored every 24 h with CCK-8 assay for 96 h. (D) RT-qPCR analysis of the knockdown efficiency for the indicated shRNAs targeting DARS1-AS1 compared with the negative control shRNA (sh-NC) in U251, U87 and LN229 cells, where GAPDH was used as an internal control. The growth of the (E) U87 and (F) LN229 cells transduced with the sh-NC/DARS1-AS1-targeting shRNAs was monitored with CCK-8 assay for the indicated time intervals. (G) RT-qPCR analysis of the knockdown efficiency for the indicated siRNAs targeting RPPH1 compared with the negative control siRNA (si-NC) in U251 and U87 cells. The growth of the (H) U251 and (I) U87 cells transfected with the si-NC/RPPH1-targeting siRNAs was monitored with CCK-8 assay for the indicated time intervals. (J) RT-qPCR analysis of the knockdown efficiency for the indicated siRNAs targeting LINC00994 compared with the si-NC in U251 and U87 cells. The growth of the (K) U251 and (L) U87 cells transfected with the si-NC/LINC00994-targeting siRNAs was monitored with CCK-8 assay for the indicated time intervals. (M) RT-qPCR analysis of DARS1 and DARS1-AS1 RNA expression in the U251 cells transfected with the si-NC or siRNAs targeting DARS1-AS1, where GAPDH was used as an internal control. (N) The 5' and 3' end sequences of DARS1-AS1 were identified by 5' RACE and 3' RACE. The corresponding PCR products were analyzed by agarose gel electrophoresis. (O) RT-qPCR analysis of the DARS1-AS1 RNA level in the U87 and U251 cells transduced with the empty lentiviral lincXpress vector (Lv-Empty) or the lincXpress vector expressing DARS1-AS1 (Lv-DARS1-AS1). Data in **A-M** are shown as mean \pm standard deviation (SD) (n=3). ** $P < 0.01$ or ns, not significant ($P > 0.05$) by 1-way ANOVA with Dunnett's multiple-comparison test. Data in **O** are shown as mean \pm SD (n=3). ** $P < 0.01$ by Student's *t*-test.

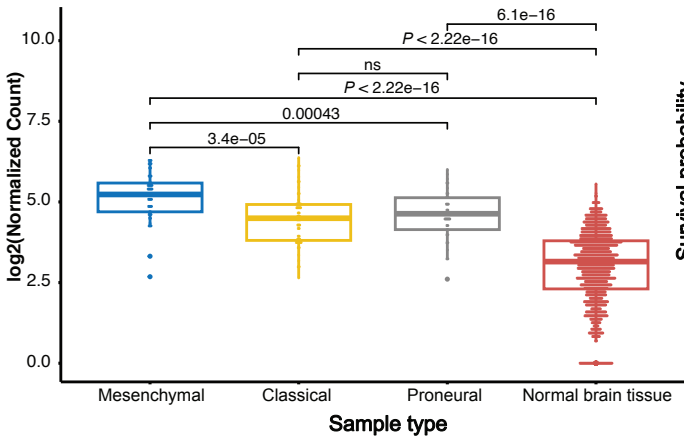
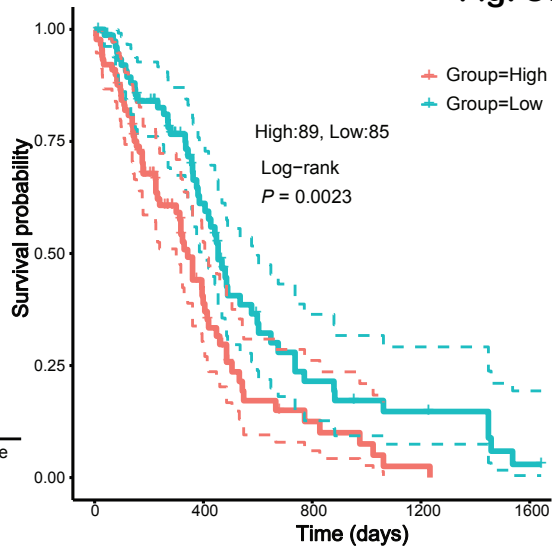
A**B****Fig. S3**

Figure S3. (A) Boxplots showing the RNA expression of DARS1-AS1 in 3 GBM subtypes (Classical, Mesenchymal and Proneural) and normal brain tissues based on TCGA and GTEx data. The statistical significance of the difference between subtypes/normal brain tissues was assessed by Wilcoxon rank-sum test; ns, not significant ($P > 0.05$). (B) Higher DARS1-AS1 expression was associated with shorter overall survival of GBM patients, based on TCGA data. The Kaplan-Meier survival curves are plotted for patient groups with high (top 50%) and low (bottom 50%) DARS1-AS1 expression in GBM tumors. The P -value was calculated using log-rank test.

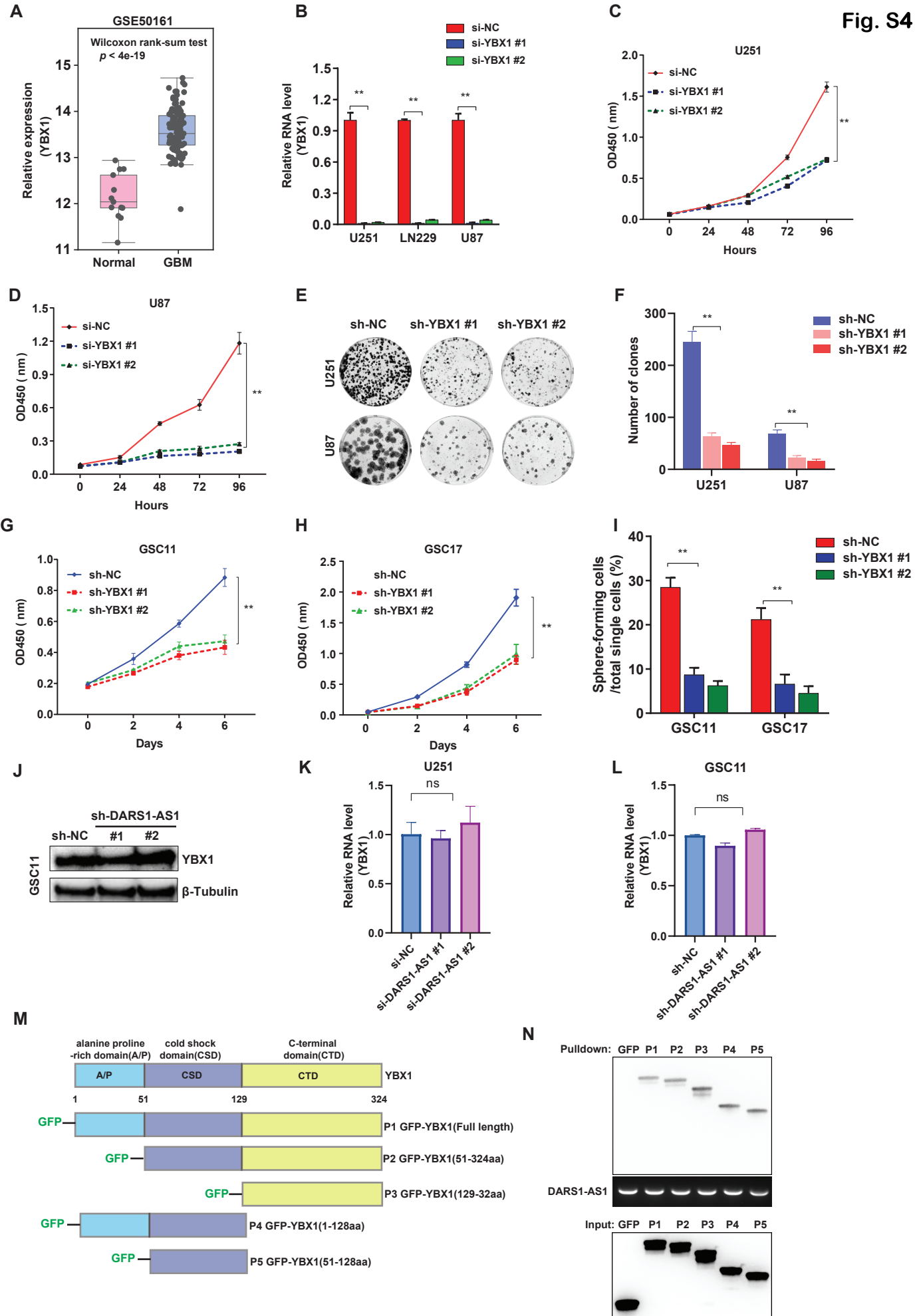


Figure S4. (A) Boxplots showing the RNA expression of YBX1 in pediatric GBM tumors and normal brain tissues based on a published gene expression profiles generated using Affymetrix HG-U133plus2 chips (GSE50161). The statistical significance of the difference in DARS1-AS1 expression between the tumors and normal brain tissues was assessed by Wilcoxon rank-sum test. (B) RT-qPCR analysis of YBX1 RNA expression in the U251, U87 and LN229 cells transfected with the negative control siRNA (si-NC) or siRNAs targeting YBX1, where GAPDH was used as an internal control. The growth of the (C) U251 and (D) U87 cells transfected with si-NC/siRNAs targeting YBX1, were monitored with CCK-8 assay for the indicated time intervals. (E) Representative pictures of clonogenic growth and (F) bar graph quantifying the colonies formed by the U251/U87 cells transduced with the negative control shRNA (sh-NC)/shRNAs targeting YBX1. The growth of the (G) GSC11 and (H) GSC17 cells transduced with sh-NC/shRNAs targeting YBX1, was monitored with CCK-8 assay. (I) The percentages of GSC11 and GSC17 cells transduced with sh-NC or YBX1-targeting shRNAs that can form neurospheres from single cells determined by self-renewal assay. (J) The protein level of YBX1 was determined by western blot in the GSC11 cells transduced with sh-NC/DARS1-AS1-targeting shRNAs, where β -tubulin was used as a loading control. RT-qPCR analysis of the RNA level of YBX1 in (K) the U251 transfected with si-NC/DARS1-AS1-targeting siRNAs or (L) the GSC11 cells transduced with sh-NC/DARS1-AS1-targeting shRNAs. (M) Schematic diagrams showing different domains of YBX1 and the GFP-tagged full-length or truncation mutant YBX1. (N) RNA pull-down coupled with anti-GFP western blot to detect the interaction between DARS1-AS1 and GFP, GFP-tagged full-length YBX1 or its truncation mutants using the cells that ectopically expressed individual proteins, wherein GFP serves as a negative control. The DARS1-AS1 retrieved from the pull-down was detected by semi-quantitative RT-PCR. Data in **B-D**, **F-I**, and **K-L** are shown as mean \pm SD (n=3). ** $P < 0.01$ or ns, not significant ($P > 0.05$) by 1-way ANOVA with Dunnett's multiple-comparison test.

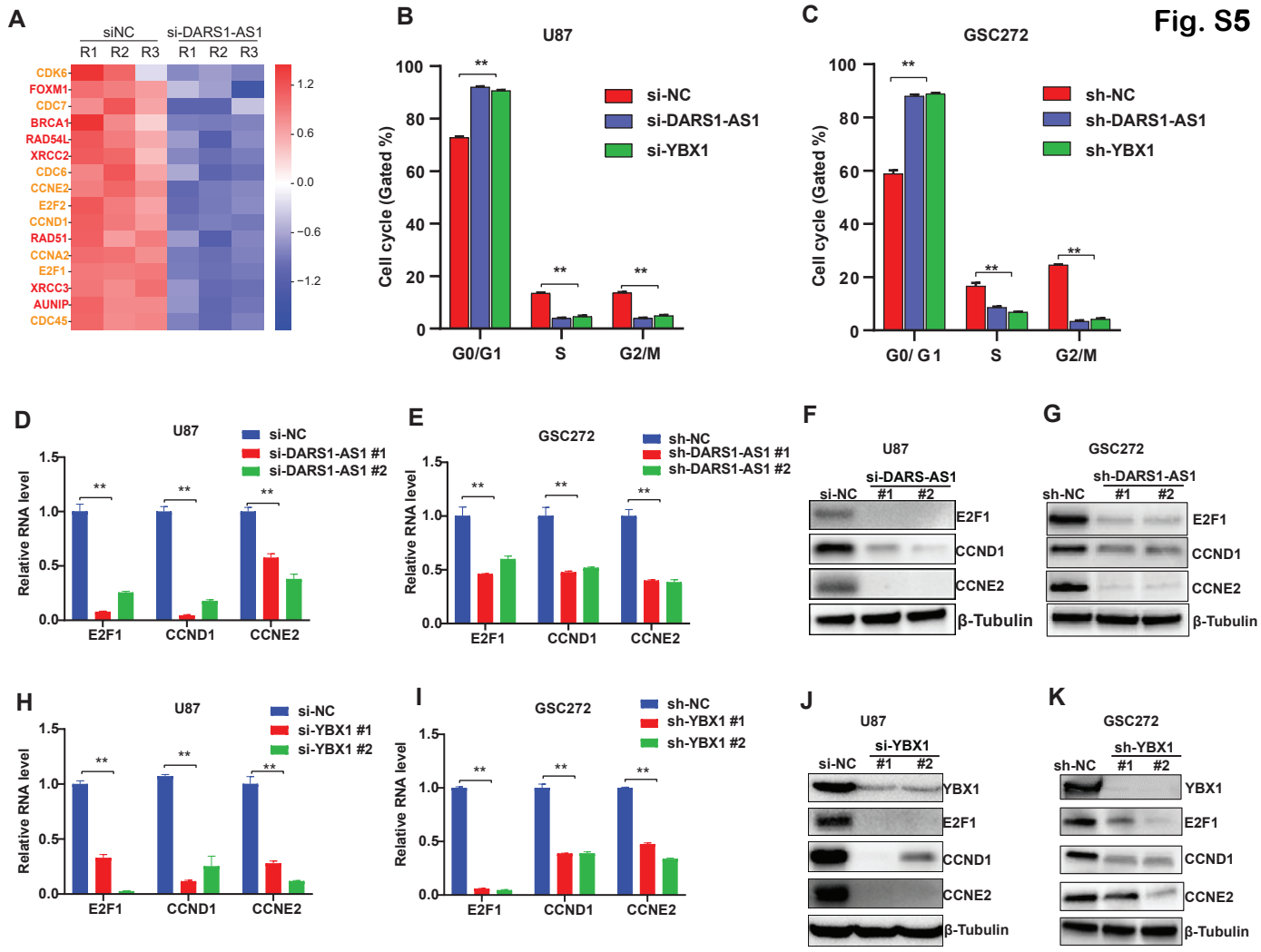


Figure S5. (A) Heatmap showing the expression of genes up-regulated by DARS1-AS1 and YBX1 (i.e., down-regulated by siRNA-mediated depletion of DARS1-AS1 and YBX1), which are associated with cell cycle (orange) or homologous recombination-mediated DNA repair pathways (red) in the U251 cells transfected with the negative control siRNA (si-NC) or DARS1-AS1-targeting siRNA. Flow cytometry based cell cycle analyses were performed for the (B) U87 and (C) GSC272 cells that were transfected/transduced with si-NC/the negative control shRNA (sh-NC) or siRNAs/shRNAs targeting DARS1-AS1 and were stained with propidium iodide. The percentages of the cells in the indicated cell cycle stages were quantified and shown in the bar graph. RT-qPCR analysis of the RNA level of the established regulators of cell cycle E2F1, CCND1 and CCNE2 in the (D) U87 and (E) GSC272 cells transfected/transduced with the negative control si-NC/sh-NC or siRNAs/shRNAs targeting DARS1-AS1. The protein level of E2F1, CCND1 and CCNE2 was determined by western blotting in the (F) U87 and (G) GSC272 cells, with/without RNAi-mediated DARS1-AS1 depletion. RT-qPCR analysis of the RNA level of the established regulators of cell cycle E2F1, CCND1 and CCNE2 in the (H) U87 and (I) GSC272 cells transfected/transduced with the negative control si-NC/sh-NC or siRNA/shRNA targeting YBX1. The protein level of E2F1, CCND1 and CCNE2 was determined by western blotting in the (J) U87 and (K) GSC272 cells, with/without RNAi-mediated YBX1 depletion. Data in **B-E** and **H-I** are shown as mean \pm SD (n=3). ** $P < 0.01$ by 1-way ANOVA with Dunnett's multiple-comparison test.

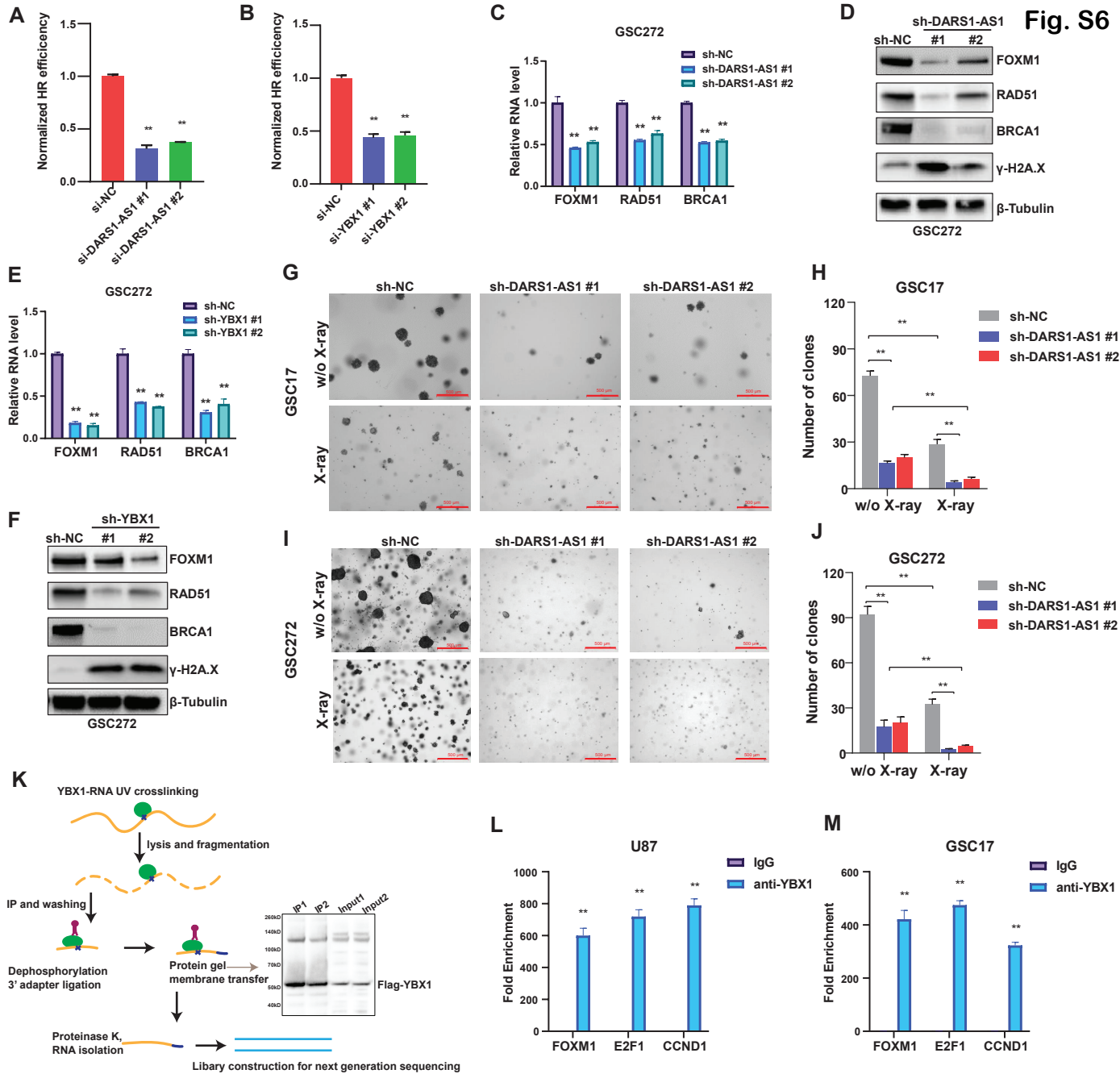


Figure S6. The effect of siRNA-mediated knockdown of (A) DARS1-AS1 or (B) YBX1 compared with the negative control siRNA (si-NC) on the homologous recombination (HR) repair efficiency was assessed using a DR-GFP reporter assay in U2OS cells (Materials and Methods). (C) RT-qPCR and (D) western blot analyses were performed to determine the RNA and protein level of the established regulator of homologous recombination-mediated DNA repair FOXM1, RAD51, and BRCA1 as well as the γ -H2AX level in the GSC272 cells transduced with sh-NC/DARS1- AS1 targeting shRNAs, respectively. (E) RT-qPCR and (F) western blot analyses were performed to determine the RNA and protein level of FOXM1, RAD51, and BRCA1 as well as the γ -H2AX level in the GSC272 cells transduced with sh-NC/YBX1 targeting shRNAs, respectively. (G) Representative pictures of soft agar colony formation and (H) bar graph quantifying the colonies formed in soft agar by the GSC17 cells that were transduced with the sh-NC or shRNAs targeting DARS1-AS1. (I) Representative pictures of soft agar colony formation and (J) bar graph quantifying the colonies formed in soft agar by the GSC272 cells that were transduced with the sh-NC or shRNAs targeting DARS1- AS1. (K) Schematic diagram of the YBX1 eCLIP-seq experiments and western blot showing the enrichment of the FLAG tagged YBX1 in the UV-crosslinked FLAG-tagged YBX1-RNA complex that was immunoprecipitated from the U251 cells in duplicate (IP1 and IP2). The whole cell lysate of the UV-crosslinked U251 cells in duplicate was used as input controls (Input1 and Input2). RNA immunoprecipitation (RIP) with an anti-YBX1/anti-IgG antibody followed by RT-qPCR validated the association of YBX1 with E2F1, CCND1 and FOXM1 mRNA in (L) U87 and (M) GSC17 cells, where anti-IgG antibody was used as a negative control. Data in **A-C** and **E** are shown as mean \pm SD (n=3). ****P** < 0.01 by 1-way ANOVA with Dunnett's multiple-comparison test. Data in **H**, **J**, and **L-M** are shown as mean \pm SD (n=3). ****P** < 0.01 by Student's *t*-test.

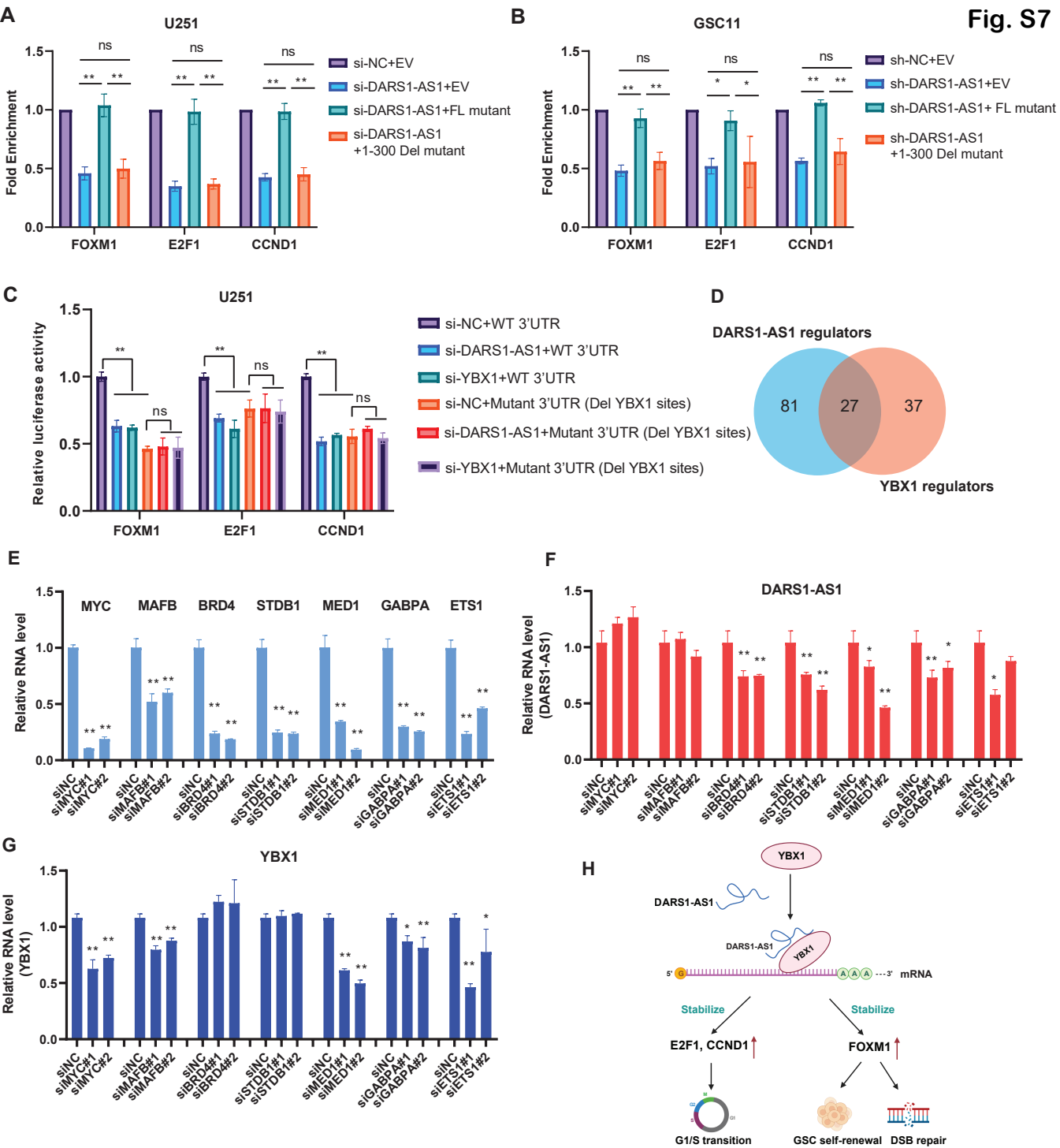


Figure S7. The fold enrichment of the YBX1 RIP signal normalized by the input on E2F1, CCND1 and FOXM1 mRNA was determined in the (A) U251 and (B) GSC11 cells that transfected with si-NC/sh-NC and empty vector (EV) or siRNA/shRNA targeting DARS1-AS1 with siRNA/shRNA resistant full length mutant /1-300 deleted mutant of DARS1-AS1. (C) Luciferase reporter assays demonstrating the binding of YBX1/DARS1-AS1 to 3'UTR of targeted mRNAs. The wild type of 3'UTR of FOXM1, E2F1, CCND1 and their YBX1 binding sites deleted mutants were cloned into downstream of promoter and luciferase transcription unit. The indicated reporter plasmid and siRNA were co-transfected into U251 cells and luciferase (firefly/Renilla) activity were measured. (D) Venn diagram showing the overlap between predicated regulators that regulate the expression of DARS1-AS1 and YBX1. (E) RT-qPCR analysis the knockdown efficiency of siRNAs targeting MYC, MAFB, BRD, STDB1, MED, GABPA and ETS1 in U251 cells. The RNA level of DARS1-AS1 (F) and YBX1 (G) in U251 cells transfected with the negative control si-NC or siRNA targeting indicated regulators. (H) Schematic diagram illustrating the mechanism of YBX1/DARS1-AS1 regulating G1/S transition, GSC self-renewal and DSB repair. Data in **A-B** are shown as mean \pm SD (n=3). ****** $P < 0.01$ or ns, not significant ($P > 0.05$) by 1-way ANOVA with Turkey's multiple-comparison test. Data in **C**, and **E-G** are shown as mean \pm SD (n=3). ****** $P < 0.01$ or ***** $P < 0.05$ by 1-way ANOVA with Dunnett's multiple-comparison test.

Supplementary Table 1. The sgRNA information and CRISPRi screen results.

Supplementary Table 2. The information about the primers, sgRNAs, siRNAs, shRNAs, and antibody.

Supplementary Table 3. The list of proteins identified by RNA pull-down followed by MS.

Supplementary Table 4. The list of differentially expressed protein-coding genes identified by RNA-seq in GBM cells upon DARS1-AS1/YBX1 knockdown, the curated gene sets (C2) from the Molecular Signature Database that were identified by GSEA as significantly enriched ones from RNA-seq data upon DARS1-AS1 knockdown, and the genes shared between GSEA and those identified by RNA pull-down followed by MS.

Supplementary Table 5. The YBX1 eCLIP-seq peaks, annotation, top enriched motifs and associated genes.

Supplementary Table 6. The list of computationally identified regulators of DARS1-AS1, YBX1 and their potential common regulators, using ChIP-seq datasets curated in Cistrome data browser, as well as the ChIP-seq datasets that provide supporting evidence for the common regulators of DARS1-AS1 and YBX1.